Behavioral/Cognitive

Alpha Oscillations Track the Projection of Reactivated Memories into Conscious Awareness

Benjamin J. Griffiths[1,2]

[1]School of Psychology, University of Nottingham, Nottingham NG7 2RD, United Kingdom and [2]Centre for Human Brain Health, University of Birmingham, Birmingham B15 2TT, United Kingdom

By definition, episodic memory is a conscious phenomenon. Memory traces reactivated by the hippocampus and reinstated in the sensory cortices need to enter conscious awareness for them to be re-experienced and overtly recalled. However, it remains unclear whether such reactivation in-and-of-itself ensures that memories will be overtly recalled. To investigate this, magnetoencephalography recordings were analyzed from 31 participants (18 females, 13 males) completing a video–word paired-associates memory task. When combining linear classifiers and spectral analyses, sensory cortical reactivation could be observed without overt recall occurring, suggesting reactivation does not guarantee overt recall. Instead, overt recall was additively predicted by (1) an increase in reactivated representations rhythmically fluctuating within the alpha band and (2) a decrease in total sensory neocortical alpha power. These results are consistent with accounts which propose that reactivation benefits from desynchronizing the network to provide representational space for stimulus-specific information and/or amplifying stimulus-specific information above residual noise. Altogether, these results suggest that representational reactivation can occur without overt recall and suggest a role for alpha oscillations in projecting internally generated representations into conscious awareness.

Key words: **alpha oscillations; consciousness; episodic memory; MEG; MVPA; reactivation**

Significance Statement

Growing evidence suggests episodic recall can occur without conscious awareness, raising a fundamental question: how do memories enter awareness? Here, we investigate whether alpha oscillatory activity relates to this process. Using magnetoencephalography, we show that while episodic memories can be reinstated in the neocortex without overt recall occurring, rhythmic reactivation within the alpha band distinguishes memories that will be recalled from those that will not, suggesting reactivation must exceed a threshold for the memory contents to enter awareness. These findings challenge the idea that memory reactivation inherently results in conscious awareness and highlight a new target for brain-based interventions aimed at improving memory in both healthy individuals and clinical populations.

Introduction

Episodic memory retrieval is a complex, multistage process that begins with the reactivation of a compressed memory trace and ends with the conscious re-experience of a past event (Teyler and Rudy, 2007; Moscovitch et al., 2016; Staresina and Wimber, 2019; Kerrén et al., 2025). The neural processes that reactivate hippocampal memory traces (Wilson and McNaughton, 1994; Gelbard-Sagiv et al., 2008; Singer and Frank, 2009; Staresina et al., 2013; Tayler et al., 2013) and reinstate them in the sensory neocortices (Bosch et al., 2014; Staresina et al., 2019; Vaz et al., 2019), collectively referred to as "reactivation" from here on, are well documented and likely necessary for us to consciously re-experience a past event (Tulving, 1985, 2002). Nonetheless, vision research shows that sensory cortical representation of a stimulus does not guarantee conscious awareness of said stimulus (Charles et al., 2014; King et al., 2016). If this generalizes to reactivated representations, it would suggest that additional neural mechanisms are required for memories to propelled into awareness.

If reactivation does not guarantee conscious access, what could? Recent studies on stimulus-specific prediction (Noah et al., 2020; Chen et al., 2023; Hetenyi et al., 2025), imagination (Xie et al., 2020; Stecher and Kaiser, 2024), and memory (Michelmann et al., 2016; Kerrén et al., 2018) implicate alpha

Received July 31, 2025; revised Feb. 13, 2026; accepted Feb. 27, 2026.

Author contributions: B.J.G. designed research; B.J.G. performed research; B.J.G. analyzed data; B.J.G. wrote the paper.

This work was supported by a Leverhulme Early Career Fellowship awarded to B.J.G. (ECF-2021-628).

The author declares no competing financial interests.

Correspondence should be addressed to Benjamin J. Griffiths at benjamin.griffiths@nottingham.ac.uk.

This paper contains supplemental material available at: https://doi.org/10.1523/JNEUROSCI.1487-25.2026

https://doi.org/10.1523/JNEUROSCI.1487-25.2026

Copyright © 2026 Griffiths

This is an open-access article distributed under the terms of the Creative Commons Attribution 4.0 International license, which permits unrestricted use, distribution and reproduction in any medium provided that the original work is properly attributed.

oscillations. These studies show that such internally generated information exhibits rhythmic fluctuations at ∼10 Hz, and this rhythmicity appears behaviorally relevant (Noah et al., 2020; Hetenyi et al., 2025), aligning with information-routing accounts proposing that alpha oscillations transmit top–down information across the cortex (Bastos et al., 2015, 2020; Stecher et al., 2025). Speculatively, therefore, alpha oscillations may route reactivated content across the hippocampus, sensory cortex, and beyond, enabling it to be acted upon and overly recalled.

Paradoxically, however, episodic memory retrieval is associated with a suppression of alpha oscillatory activity (Michelmann et al., 2016; Staresina et al., 2016; Waldhauser et al., 2016; Griffiths et al., 2019b; Karlsson et al., 2020; Martín-Buro et al., 2020; Griffiths et al., 2021; Katerman et al., 2022), which is theorized to increase representational space for stimulus processing (Hanslmayr et al., 2012; Jensen et al., 2012). One resolution to this paradox incorporates a stimulus-specific synchronization component, which amplifies stimulus-specific information above residual "noise" that was not desynchronized (Griffiths et al., 2019a; Michelmann et al., 2022). This enables the network to communicate by either desynchronizing stimulus-irrelevant assemblies or synchronizing stimulus-specific assemblies, thereby elevating the signal above background noise. While stimulus-specific synchronization is likely masked by the desynchronization of stimulus-irrelevant assemblies in macroscopic sensor data, classifiers combined with spectral methods can isolate these dynamics (Kerrén et al., 2018, 2023; Hetenyi et al., 2025), enabling us to investigate whether (1) alpha rhythmicity in stimulus-specific representations co-occurs with more general alpha power decreases and (2) they interact to during conscious access of a reactivated memory.

Conscious experience of memories is often measured using subjective measures such as vividness or confidence (Simons et al., 2010; Thakral et al., 2015; Kerrén et al., 2024), which assess the intensity of experience but require the memory to have emerged into awareness. In contrast, objective, overt report (commonly used in visual perceptual studies of consciousness) may offer a more direct measure of conscious access. While some argue that overt recall cannot capture richness of experience (Tsuchiya et al., 2015), this issue is moot for categorical memory tests (e.g., forced-choice cued recall), where failure to report can only arise due to motor or response errors. Consequently, categorical recall offers a proxy for awareness that requires the stimulus to come to mind without requiring further complex cognitive operations to complete the report. Here, we use this measure to determine whether the reactivation of sensory representations guarantees overt recall of episodic memories and, if not, what predicts whether reactivated episodic memories will be overtly recalled.

Materials and Methods

Dataset. The dataset was taken from a recent study investigating the impact of high-frequency (>34 Hz) rhythmic light stimulation on the brain and cognition (Griffiths et al., 2025). This stimulation was delivered during encoding and retrieval, producing neural responses in the target gamma frequencies, but no effects were observed in frequencies below 34 Hz. All spectral analyses here focus on rhythmic fluctuations at 30 Hz and below.

Participants. Thirty-seven participants were recruited [mean age, 24.7; age range, 18–37; 64.9% female; all right-handed (self-reported)]. This sample size was selected to achieve sufficient power for the original project (Griffiths et al., 2025). Nonetheless, it is sufficiently powered for detecting neural representations during recall, providing a sample size similar to other retrieval-focused decoding studies (Michelmann et al., 2016; Kerrén et al., 2018; Linde-Domingo et al., 2019). Participants were compensated with course credit or cash payment. Participants provided informed consent before starting the experiment. Ethical approval was granted by the Research Ethics Committee at the University of Birmingham.

Behavioral task. Participants completed a paired-associates episodic memory task, learning 192 video–word pairs across three blocks (Michelmann et al., 2016). During encoding, each trial began with a fixation cross (1.5 ± 0.2 s jitter), followed by a video clip and then an English noun (both presented for 3 s). There were four videos in total, each paired to 48 nouns. Videos were presented in a pseudorandomized order so that each video would appear twice every eight trials. After encoding the video–word pair, participants reported whether they could perceive the rhythmic light stimulation as a flicker on the screen during stimulus presentation. Participants had 3 s to respond using the keyboard before the next trial began. This task was used to keep participants attending to the screen during the block.

Participants then completed a short (∼2 min) distractor task. They were presented with a sum on the screen and had to choose between two possible answers. If participants selected incorrectly, they had to redo the sum. The task ended after participants had completed at least 10 sums and after 2 min had elapsed.

After being exposed to all pairs of a block, participants completed a retrieval test. During retrieval, each trial began with a fixation cross (1.5 ± 0.2 s jitter), followed by an English noun (presented for three seconds). These nouns were taken from the immediately preceding encoding phase. Participants had 3 s to select which of the four videos they thought was associated with the word. Following this, a prompt asked whether the participant felt they were confident in their response. Again, participants had 3 s to provide a binary answer ("yes" or "no"). This task can be considered a hybrid of cued recall and recognition: participants are given a cue to recall the stimulus (as in cued recall) and then asked to select the target from a lineup (akin to recognition). However, as representational analysis was restricted to the presentation of the cue (i.e., before the lineup) and therefore any identified representation must have been recalled from memory, the following analyses better capture the dynamics of recall rather than recognition.

Behavioral analysis focused on objective, overt recall. That is, whether the participant selected the correct stimulus regardless of how confident they felt about their decision.

MEG acquisition and preprocessing. Magnetoencephalography (MEG) was recorded using a 306-channel MEGIN Elekta Triux system, with a 1,000 Hz sampling rate. Data were preprocessed using MNE Python (Gramfort, 2013) following the FLUX pipeline (Ferrante et al., 2022). The raw data were corrected using Maxwell filters, with bad channels being marked and removed. Data were then bandpass filtered between 0.5 and 220 Hz, with notch filters at 50, 100, 150, and 200 Hz to attenuate line noise. Muscle artifacts were detected automatically using MNE's *annotate_muscle_zscore*, identifying activity between 110 and 140 Hz that exceeds a *z*-score of 10. Following this, independent component analysis (ICA) was used to remove spatially stable artifacts (e.g., blinks, saccades). Muscle artifact and bad channel detection were repeated after ICA to remove residual noise. Bad channels were then interpolated using the average of neighboring electrodes. Finally, the data were epoched around stimulus onset (encoding, video onset; retrieval, noun onset), starting 2 s before stimulus onset and ending 2 s after stimulus offset.

Structural MRI acquisition. Anatomic images were acquired for all but two participants using a 3 T Siemens Magnetom Prisma scanner (T1-weighted MPRAGE; TR, 2,000 ms; TE, 2.01 ms; TI, 880 ms; flip angle, 8°; FOV, 256 × 256 × 208 mm; isotropic voxels, 1 mm). The remaining two participants could not be contacted to return for the MRI, so we used the Colin27 template for these individuals (Holmes et al., 1998).

MEG source analysis. To compute the source model, we aligned the coordinate system of the participants' individual T1 scans to the anatomic landmarks and digitized the scalp shapes before the recordings. The T1 was then aligned to the MEG using four digitized head position

indicator coils. A single shell boundary elements model was constructed based on the brain surface using FreeSurfer (Dale et al., 1999; Destrieux et al., 2010). This was then used to construct a volumetric forward model (10 mm grid) and lead field matrix covering the whole brain. A linearly constrained minimum variance beamformer was then applied to the sensor-level amplitude time-series. The beamformer was created using MNE's *mne.beamformer.make_lcmv*, with a data covariance matrix taken from the 3 s of data following stimulus presentation and a noise covariance matrix taken from −1.5 s to −1 s prior to stimulus onset (avoiding 1 s of rhythmic light stimulation before the cue appeared). This returned a filter which was applied to each trial individually. This returned a source-space representation of the MEG data that was analyzed in the same manner as its sensor-level counterpart, ensuring no localization differences could arise between different analyses [e.g., linear-discriminant analysis (LDA) and time–frequency analysis].

Participant exclusion. Participants were excluded either because (1) their MEG contained large artifacts that could not be suppressed using the preprocessing pipeline above ($n = 2$) or (2) they had either too few (i.e., <30) remembered or forgotten trials to get a reliable estimate of the neural correlates associated with these behaviors ($n = 4$). This left 31 participants in the final sample [mean age, 24.8; age range, 18–37; 58.1% female; all right-handed (self-reported)].

Cross-validated perceptual decoding. Multiclass time-generalized LDA was used to classify sensor-level MEG activity as relating to one of the four videos. First, the data were low-pass filtered at 100 Hz and (then) downsampled to 200 Hz. Second, the data were baseline-corrected trialwise by subtracting from the mean amplitude between 250 and 50 ms prestimulus from all timepoints. Third, the sensor-level MEG was decomposed into the 40 principal components that explained most variance in the data. This limit was driven by MaxFilter, which reduces the rank of the data to ∼60 components (but this varies from participant to participant). Using 40 components ensures that no participant has rank-deficient data entered into the LDA analysis. Across participants, these 40 principal components on average explained 95.1% of the data. Fourth, the data was re-epoched from 250 ms prestimulus to 1,000 ms poststimulus (removing filter-induced edge artifacts). Fifth, the data were *z*-scored across principal components. Sixth, the data were split into fivefolds, with each fold containing data from every fifth trial, such that the first fold contained Trials 1, 6, 11, 16, etc.; the second fold contained Trials 2, 7, 12, 17, etc.; and so on. This was done across recalled and not-recalled items to ensure there were no condition-specific differences in the training dataset that might drive later results (e.g., some images being more memorable than others; Kyle-Davidson et al., 2022). Seventh, for a given MEG sample, the classifier [scikit-learn's LDA (Pedregosa et al., 2011) with the "eigen" solver and automatic shrinkage using the Ledoit–Wolf lemma] was trained to distinguish between the four videos using four of these folds. Eighth, the classifier trained on one timepoint was applied to every timepoint of the held-out fifth fold, with decision values being used as the measure of classifier performance. Ninth, this process was repeated for every timepoint in the training dataset to build a time-generalization matrix of decoding performance and repeated in a cross-validated manner so that each fold acted in turn as the test data, with the resulting decision values for each repetition being averaged to provide a single time-generalization matrix of classifier performance.

While chance performance for LDA using decision values should theoretically be zero, hidden biases in the data may distort this. To remedy this, we empirically defined chance performance by repeating the pipeline as above 100 times with a single alteration: that the labels (i.e., the video identities) were shuffled randomly during the training of the LDA classifier. This produced 100 decoding time-series that would be expected to emerge by chance. The median and median absolute deviations of these time-series were computed (per sample) and then used to normalize the "true" decoding time-series computed above. This meant that chance performance for the "true" decoding time-series was now known to be zero, with the unit measurement being median absolute deviations from chance.

These steps were repeated for each participant, and the resulting data were pooled for inferential statistical analysis. To this end, a cluster-based one–sample permutation *t* test (1,000 permutations; as in Maris and Oostenveld, 2007) was conducted to determine whether normalized decision values, pooled across participants, significantly differed from the chance-level surrogate distribution ($p < 0.05$).

Generalized decoding from perception to retrieval. The LDA approach used above was expanded to search for the reactivation of video information during the recall phase of the experiment. The encoding and retrieval data were baseline-corrected, converted to principal components, downsampled, and normalized as above. The encoding epochs were again re-epoched from 250 ms prestimulus to 1,000 ms poststimulus, whereas the retrieval epochs were re-epoched from 250 ms prestimulus to 3,000 ms poststimulus (accounting for delays in the reactivation process; Staresina and Wimber, 2019). From here, the LDA classifier was trained on data from the encoding epochs and then tested on data from the retrieval epochs, doing so in a time-generalized manner. This process was repeated three times: once using all retrieval trials, once using retrieval trials that exhibited overt recall, and once using retrieval trials that did not exhibit overt recall. As above, this whole procedure was then repeated 100 times using classifiers that had been trained on shuffled labels, with the "true" decoding performance being normalized using the median and median absolute deviation of this surrogate distribution.

The resulting data were pooled across participants for inferential statistical analysis. To this end, one cluster-based one–sample *t* test (1,000 permutations; as in Maris and Oostenveld, 2007) was conducted to determine whether normalized decision values across all trials, pooled across participants, was significantly greater than the chance-level surrogate distribution ($p < 0.05$). A second cluster-based paired–sample permutation *t* test (1,000 permutations) was conducted to determine whether normalized decision values for recall trials was significantly greater than normalized decision values for forgotten trials ($p < 0.05$).

Peak-locked analysis of retrieval decoding. The onset of memory reactivation is more temporally variable than other cognitive phenomena often subjected to classification-based analyses (Staresina and Wimber, 2019). Therefore, standard stimulus-locked decoding analyses may understate or mask key neural dynamics of memory reactivation (Van Bree et al., 2024). To address this issue, we used peak-locking—an approach that aligns trials based on local maxima in brain activity rather than aligning them to an external stimulus.

To this end, we conducted a similar decoding approach to that above, Generalized decoding from perception to retrieval, up until the point where a decoding time-series for the retrieval data was computed. At this stage, we began the peak-locking procedure. For a given trial and for a given generalized timepoint from the encoding time-series, we detected the timepoint in the retrieval time-series where decoding peaked. The trial decoding time-series was re-epoched using this maximum, beginning 500 ms before the moment of peak decoding and ending 500 ms after. We repeated this process for every trial and averaged over trials to provide the peak-locked average (this was done for the three memory conditions separately, i.e., all trials; remembered only; forgotten only). This process was repeated for each timepoint in the encoding time-series to generate a time-generalization matrix from stimulus-locked encoding data to peak-locked retrieval data.

As we lock the data to the maximum of each trial, classifier performance will be above zero, even for chance data. Therefore, we again used surrogate distributions to estimate what chance performance would be when using this procedure. This matched how it was done in the previous sections: that is, we shuffled training labels. The "true" peak-locked average was then normalized using the median and median absolute deviation of the surrogate distribution, such that zero once again reflected decoding performance expected by chance. Simulations indicate that this corrects the peak-locking bias (Fig. S1).

The peak-locked averages were pooled across participants for inferential statistical analysis conducted in the same manner as above, Generalized decoding from perception to retrieval: one cluster-based one–sample permutation *t* test (1,000 permutations; Maris and

Oostenveld, 2007) was conducted to determine whether normalized decision values across all trials, pooled across participants, was significantly greater than the chance-level surrogate distribution ($p < 0.05$). A second cluster-based paired–sample permutation t test (1,000 permutations) was conducted to determine whether normalized decision values for recall trials were significantly greater than normalized decision values for forgotten trials ($p < 0.05$).

Spectral power analysis of retrieval decoding. Spectral power analysis was conducted on the normalized peak-locked averages. The peak-locked averages were transformed into a time–frequency representation using Morlet wavelets spaced 0.25 Hz apart, from 2 and 40 Hz, with a cycle length of half of the desired frequency (e.g., power at 10 Hz was computed using wavelets of five cycles). This was done for all three memory conditions, for every timepoint of the decoding peak-locked average, and for every timepoint of the generalization from encoding. The power spectra were averaged across all timepoints (both at encoding and retrieval) as the information contained in each individual timepoint was largely redundant, and the estimation of the 1/f in the following step benefits from averaging over samples (Miller et al., 2009; Griffiths et al., 2019a). The 1/f curvature of the power spectra was computed and subtracted from the raw power spectra using *specparam* (Donoghue et al., 2020). This meant that any power value greater than zero could be linked to specific increases in narrowband oscillatory activity, rather than broadband, aperiodic fluctuations.

The power spectra were pooled across participants for inferential statistical analysis conducted in the same manner as above, Generalized decoding from perception to retrieval: one cluster-based one–sample permutation t test (1,000 permutations) was conducted across all timepoints and frequencies to determine whether 1/f-corrected power spectra across all trials contained peaks in activity that was significantly greater than what was present in aperiodic component ($p < 0.05$), indicating the presence of narrowband oscillatory rhythmicity in the peak-lock average. A second cluster-based paired–sample permutation t test (1,000 permutations) was conducted across all timepoints and frequencies to determine whether the power spectra of decision values for recall trials were significantly greater than the power spectra of decision values for forgotten trials ($p < 0.05$).

To rule out the possibility that decoding effects were driven by stimulus memorability, this analysis was repeated after resampling the trials so that all stimulus*memory combinations (video1*remembered, video1*forgotten, video2*remembered, etc.) are balanced for a given participant and then shuffling the stimulus labels within memory conditions (i.e., labels could be shuffled between "video1*remembered" and "video2*remembered" but not between "video1*forgotten" and "video2*remembered). All other steps of the analysis were unchanged.

Source-level searchlight LDA. For source-level searchlight analyses, decoding was conducted by first reconstructing the amplitude time-series for every virtual sensor and then conducting LDA on these virtual sensors. All steps matched those described above with one exception: rather than using PCA, the dimensionality of the data was reduced by restricting analysis to a single voxel and its immediate neighbors (using MNE's *spatial_src_adjacency*). This process was repeated iteratively for every voxel of the source data to build a 3D source volume of decision values for each participant individually. These source maps were morphed into a common space using the standard FreeSurfer average. For statistical analysis, one cluster-based one–sample permutation t test (1,000 permutations) was conducted across all searchlights to determine whether 1/f-corrected power spectra across all trials contained peaks in activity that were significantly greater than what was present in the aperiodic component ($p < 0.05$). A second cluster-based paired–sample permutation t test (1,000 permutations) was conducted across all searchlights to determine whether the power spectra of decision values for recall trials were significantly greater than the power spectra of decision values for forgotten trials ($p < 0.05$).

Time–frequency analysis of MEG amplitude. Time–frequency analyses of amplitude were first conducted on stimulus-locked data. The data were downsampled to 500 Hz. Morlet wavelets were used to compute spectral power at 39 equidistant frequencies between 2 and 40 Hz. The length of these wavelets was half of their frequency (i.e., power at 10 Hz was computed using wavelets of five cycles). For each memory condition (all trials; remembered only; forgotten only), the spectra were averaged across trials. The 1/f curvature was then removed from each timepoint of the power spectra using *specparam* (Donoghue et al., 2020) and split into two conditions, prestimulus and poststimulus, each of which were averaged over time.

The power spectra were pooled across participants for inferential statistical analysis. First, a cluster-based paired–sample permutation t test (1,000 permutations) was conducted to determine whether alpha power had decreased significantly poststimulus relative to prestimulus across all trials ($p < 0.05$). Second, a cluster-based paired–sample permutation t test (1,000 permutations) was conducted across all timepoints and frequencies to determine whether poststimulus power had decreased significantly for remembered relative to forgotten trials (i.e., the retrieval success effect; $p < 0.05$).

This process was repeated for time–frequency representations that had been re-epoched around the peak of decoding. This re-epoching was done in the same manner as reported above, Peak-locked analysis of retrieval decoding. Statistics match those of the preceding paragraph, but rather than considering pre- and poststimulus, the analyses instead focused on pre- and postpeak activity.

Linear modeling of the effects of decoding alpha and global alpha on memory performance. For every participant, we computed mean memory performance (i.e., the percentage of correct overt recalls), memory-related alpha–band decoding performance (i.e., the difference in alpha-band power for decoding decision values for remembered relative to forgotten trials), and memory-related alpha–band global power (i.e., the difference in alpha-band power of raw amplitude for remembered relative to forgotten trials). For both the decoding and global power measures, we averaged power across the entire epoch to avoid arbitrary windowing decisions. We then entered these into a multiple linear regression model which sought to predict memory performance based on these alpha measures and their interaction. A predictor was said to significantly relate to memory performance when the p value was smaller than 0.05.

Results

Episodic memory reactivation without overt recall

Thirty-one participants undergoing MEG completed a simple associative memory task (Fig. 1*A*). These data were taken from a recent study investigating the impact of rhythmic light stimulation on neural responses and behavior (Griffiths et al., 2025; see Materials and Methods for details). They encoded a series of video–word pairs and then, later, recalled the videos using the words as cues (Michelmann et al., 2016). On average, participants recalled 60.6% of the pairs (SD = 19.2%).

To identify memory reactivation in the neural data, we paired LDA with peak-locking procedures (Fig. 1*B*). Recent theoretical and empirical work (Staresina and Wimber, 2019; Van Bree et al., 2024) suggests that memory reactivation is temporally variable and therefore difficult to detect in cue-locked data. Peak-locking procedures circumvent this problem by aligning the time-series of individual trials to the moment when maximal decoding of the target occurs. To achieve this, classifiers were trained on the stimulus-locked encoding data (i.e., when they watched the video) and then tested on the stimulus-locked retrieval data in a time-generalized manner. For every retrieval trial, the time-generalization matrices are aligned to the maximal decision value produced by the classifier. To minimize biases that would be introduced by differences in trial numbers between hits and misses or by specifically focusing analysis on peaks of maximal decoding (Kriegeskorte et al., 2009), peak-locked time-series

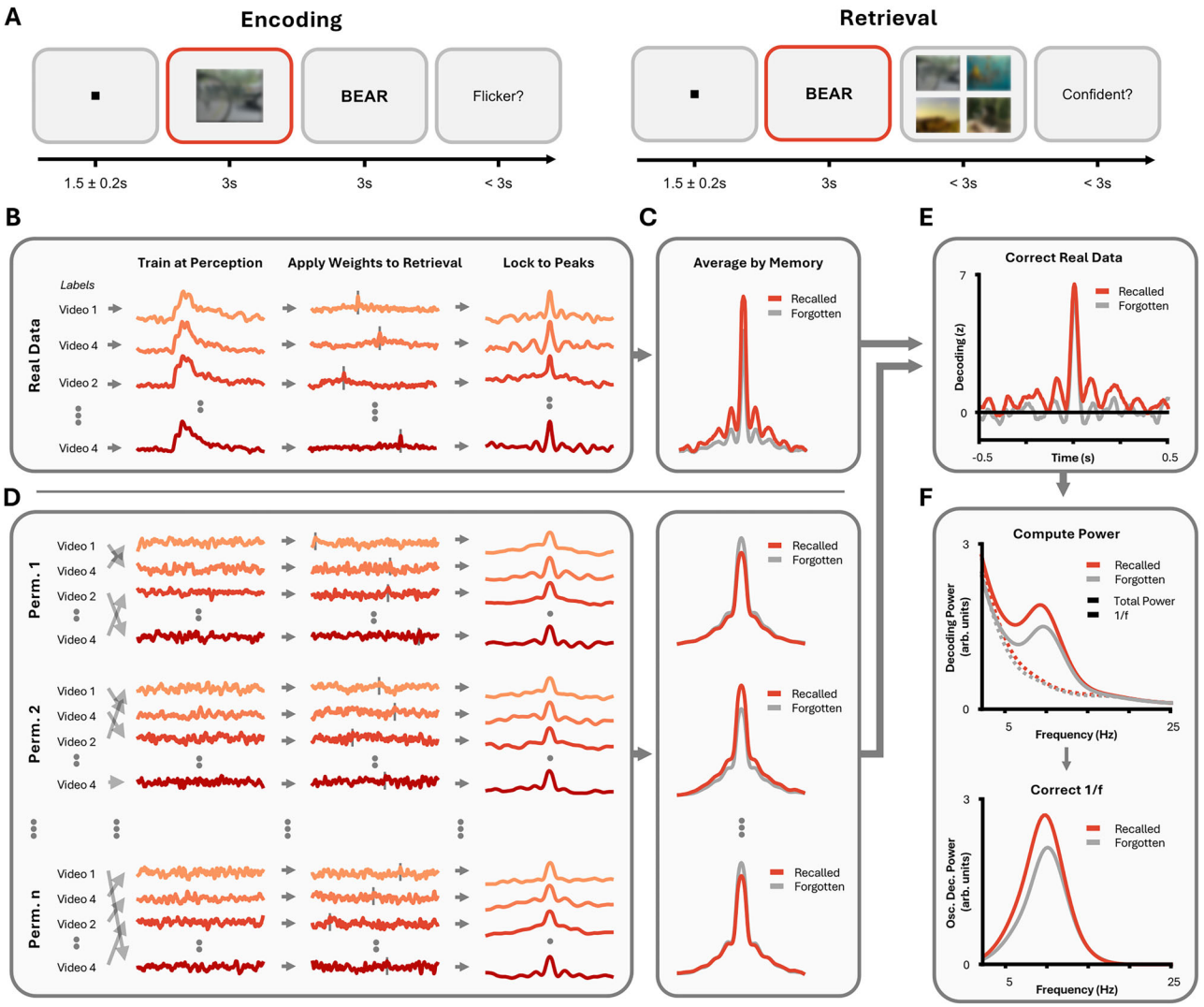


Figure 1. Methodological and analytical approach. ***A***, Behavioral task. Participants completed a paired-associates task. During encoding, they were asked to vividly associate a video with a word and then report whether they perceived a flicker on the screen. During retrieval, participants were shown the word and asked to recall the associated video. They then reported whether they were confident in their choice or not. (Video stills are blurred for copyright reasons; participants viewed unblurred videos). ***B***, We used LDA to detect the reemergence of stimulus-specific information during memory retrieval. The classifier was trained on MEG activity recorded while participants viewed the videos and was then applied to MEG activity recorded as participants attempted to recall these videos. We re-epoched the resulting decoding time-series around the point of maximal decoding (dotted lines on middle plot) on a trial-by-trial basis. ***C***, The peak-locked data were split based on memory performance, and averaged across memory-specific trials. ***D***, This process was repeated 100 times using shuffled training labels to determine the peak-locked average expected by chance. ***E***, The "true" (i.e., unshuffled) data were then normalized by subtracting the median of the "chance" (i.e., shuffled) data and dividing by its median absolute deviation. ***F***, Morlet wavelets were applied to the normalized peak-lock average and the 1/*f* was subtracted.

are normalized using a surrogate distribution of decoding scores computed by shuffling training labels. All following analyses focus on these normalized decoding scores, where chance performance is zero.

While the classifier could robustly decode stimulus content during perception above what would be expected by chance ($z = 16.38$; $p < 0.001$; Fig. 2*A*), there was no evidence for stimulus-specific content in the cue-locked retrieval data ($z = 0.05$; $p = 0.299$; Fig. 2*B*; aligning with the idea that temporal variability impedes the detection of reactivation in cue-locked data). In contrast, for the peak-locked average, reactivation was found to be significantly greater than what would be expected by chance across all trials ($z = 23.64$; $p < 0.001$; Fig. 2*C*). Critically, when splitting trials based on memory performance, decoding proved to be significantly greater than chance for both remembered and forgotten stimuli (recalled, $z = 24.26$; $p < 0.001$; not recalled, $z = 21.28$; $p < 0.001$). Notably, there was no difference in decoding magnitude between remembered and forgotten stimuli ($z = 0.06$; $p = 0.177$). Taken together, these results suggest that accurate memory reactivation can occur without overt recall.

To investigate whether alpha oscillations act as a bridge between reactivation and overt recall, the power spectrum of the peak-locked average was computed and normalized against the exponent of the spectrum, such that an increase in power above zero indicated narrowband power above what could be explained by the exponent itself. A significant increase in narrowband power was observed across all trials ($z = 29.19$; $p < 0.001$; Fig. 2*D*), peaking at ~10 Hz, suggesting the reactivated representations fluctuate rhythmically within the alpha band. This was true when analyzing remembered and forgotten stimuli separately (recalled, $z = 24.37$; $p < 0.001$; not recalled, $z = 25.70$; $p < 0.001$) but, critically, was significantly greater for remembered relative to forgotten items ($z = 3.67$; $p = 0.015$; Fig. 2*E*). These results suggest that the rhythmicity of reactivation, rather than

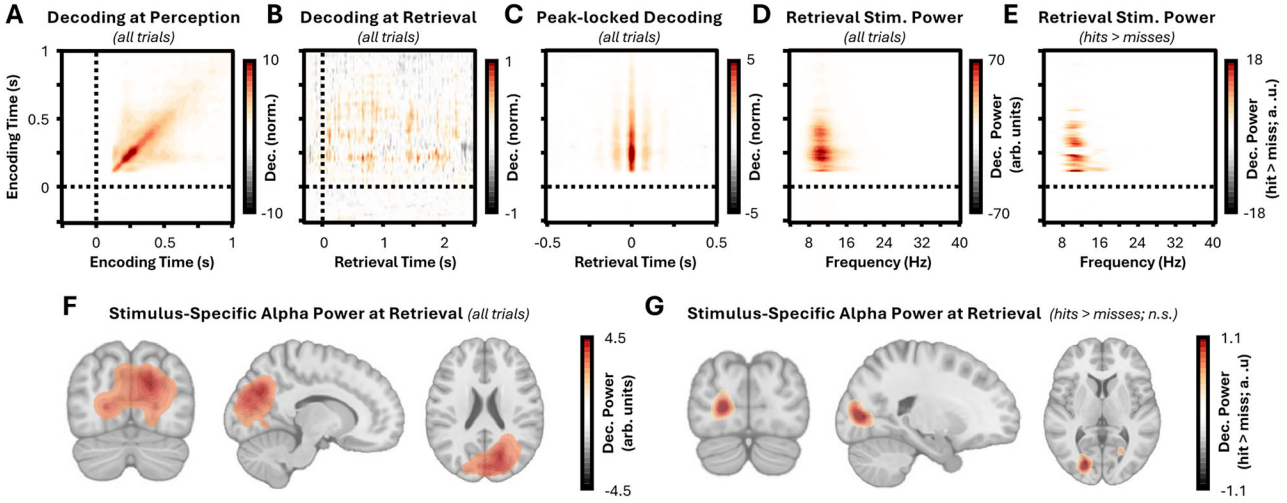


Figure 2. Episodic memory reactivation occurs without overt recall. ***A***, Time generalization of LDA on encoding data across all trials. Stimulus-specific content could be reliably decoded from MEG data during the viewing of videos from ∼200 ms after stimulus onset. Training time is presented on the *y*-axis; testing time is presented on the *x*-axis. The color bar depicts decoding performance relative to chance (shuffled label) data. ***B***, Time generalization of LDA from encoding to cue-locked retrieval data, across all trials. There was no reliable decoding of stimulus content in the retrieval data when the MEG was locked to cue onset. The classifier was trained on data from encoding (*y*-axis) and applied to the retrieval time-series (*x*-axis). The color bar as in Panel ***A***. ***C***, Time generalization of LDA from encoding to peak-locked retrieval data, across all trials. Rhythmic patterns in the decoding of stimulus content could be observed in the broadband amplitude time-series for the retrieval data when the MEG was locked to peaks. The classifier was trained on data from encoding (*y*-axis) and applied to the retrieval time-series (*x*-axis). The color bar as in Panel ***A***. ***D***, Power spectrum of peak-locked LDA across all trials. Taking the time-generalization matrix from Panel ***C***, 1/*f* corrected power was computed for each training time point (*y*-axis) for frequencies between 2 and 40 Hz (*x*-axis). Color bar depicts narrowband decoding performance relative to the 1/*f* curve. ***E***, Memory-related changes in decoding power. The power spectra for hits and misses were contrasted to identify whether rhythmic reactivation predicted overt recall for training timepoints (*y*-axis) or frequencies between 2 and 40 Hz (*x*-axis). The color bar depicts narrowband decoding performance for remembered relative to forgotten items. ***F***, Source localization of α-band rhythmic reactivation across all trials. Searchlight-based decoding revealed that decoding was strongest over occipital areas. Voxels with values between 25% of the color bar minimum and 25% of the color bar maximum (here, $-1.13 < \text{voxel} < 1.13$) are masked. ***G***, Source localization of alpha-band rhythmic reactivation for remembered relative to forgotten stimuli. Searchlight-based decoding revealed that recall-related decoding was again strongest over occipital areas, though this difference was not significant. Voxels with values between 25% of the color bar minimum and 25% of the color bar maximum (here, $-0.28 < \text{voxel} < 0.28$) are masked.

its raw magnitude, distinguishes between memories that will be overtly recalled and those that will not.

Notably, while these results demonstrate that reactivated content fluctuates within the alpha band, this does not necessarily mean that the content is represented in alpha oscillations. As the analysis was conducted on broadband time-series, it is possible that these rhythmic increases in decoding are a result of other neural dynamics that emerge at specific phases of alpha oscillations (e.g., alpha–gamma coupling; Jensen et al., 2012). To rule out this possibility, the analyses in the paragraph above were repeated using narrowband-filtered data from 6 to 14 Hz. This approach produced the same outcomes as above, namely, that representations of remembered and forgotten stimuli both rhythmically fluctuate within the alpha band (recalled, $z = 26.59$; $p < 0.001$; not recalled, $z = 26.57$; $p < 0.001$), but this rhythmicity was greater for hits relative to misses ($z = 9.35$; $p < 0.001$; Fig. S2).

To identify which brain regions supported these reconstructed representations, the decoding effects were source localized using searchlights. Across all trials, cluster-based permutation tests revealed rhythmic decoding ($z = 20.46$; $p < 0.001$; Fig. 2*F*), peaking in occipital and inferior parietal regions. Intriguingly, however, no region showed differences in decoding between recalled and forgotten items ($z = -0.70$; $p = 0.798$; Fig. 2*G*). Given that across-sensor classification analysis of rhythmic representations can predict overt recall but searchlight analyses cannot, it would suggest that global, not local, representations of stimulus-specific content predict overt recall.

An alternative account of the observed rhythmic reactivation is that the decoding reflects a general memory effect rather than stimulus-specific information. As the classifier was trained on encoding data, it cannot learn retrieval-specific patterns. However, it could still pick up on stimulus features that make certain videos inherently more memorable (Bainbridge et al., 2025), which could still bias the results. To address this, trial numbers for all label-by-memory combinations were balanced within participants, and all label shuffling was conducted within memory conditions. These additional controls did not impact the main results, with both recalled and forgotten items producing significant alpha rhythmic decoding (recalled, $z = 24.278$; $p < 0.001$; forgotten, $z = 20.951$; $p = 0.001$) and a memory-related difference in alpha rhythmic reactivation existing between the two conditions ($z = 3.006$; $p = 0.023$).

A second alternative account is that participants reactivate all possible responses iteratively in a rhythmic fashion. If true, the magnitude of rhythmic decoding should be approximately equivalent for each of the four stimuli. In contrast, if participants selectively reactivate the target stimulus, then evidence for this should be substantially greater than evidence for any of the other stimuli (for visual depiction of hypotheses, see Fig. S3). When testing this idea, rhythmic decoding was found to be significantly greater for the target stimulus relative to the other stimuli, for both recalled and forgotten items (recalled, $z = 21.43$; $p = 0.001$; not recalled $z = 20.76$; $p = 0.001$; Fig. S3), suggesting participants reactivate the target stimulus rather than iterating through all possible outcomes.

Altogether, these results suggest that episodic memories can be reactivated within the sensory neocortex in the absence of overt recall. Instead, overt recall is predicted by the degree of alpha rhythmic reactivation, suggesting that alpha oscillations may track conscious access to reactivated memories.

Total alpha power decreases predict overt recall of reactivated memories

Given the large body of work linking alpha power decreases to successful memory retrieval (Staresina et al., 2016; Waldhauser

et al., 2016; Karlsson et al., 2020; Martín-Buro et al., 2020; Griffiths et al., 2021; Katerman et al., 2022), including three datasets using the same paradigm as here (Michelmann et al., 2016; Griffiths et al., 2019a,b), we asked whether memory-related alpha power decreases also arise in this dataset. Morlet wavelets were applied to the raw, cue-locked MEG data and then subtracted the exponent from the resulting power spectrum to provide a measure of narrowband alpha power (to aid distinction from the decoding analyses, this measure is referred to as "total alpha power," while any reference to the decoding measure used in the previous section is referred to as "stimulus-specific rhythmic reactivation"). Total power for both remembered and forgotten stimuli decreased significantly following the presentation of the cue ($z = -13.76$; $p < 0.001$; Fig. 3*A*) over similar regions to those observed for the decoding effects (Fig. 3*E*). Importantly, this decrease was substantially greater for remembered relative to forgotten items ($z = -5.46$; $p = 0.005$; Fig. 3*B*,*F*), demonstrating that memory-related decreases in total alpha power matched those observed in previous studies.

Repeating these analyses after locking the raw data to the moment of maximal reactivation (as detected in the decoding analyses) produced similar results: there was a significant decrease in total power following the moment of maximal decoding ($z = -5.46$; $p = 0.005$), and total power was significantly lower for remembered relative to forgotten items ($z = -7.57$; $p = 0.002$; Fig. 3*C*). Notably, there was no interaction between memory performance and total power before and after the decoding peak ($F_{(1,30)} = 0.52$; $p = 0.476$; Fig. 3*D*). This suggests that total alpha power across the retrieval attempt, rather than only after reactivation, predicts overt recall. This suggests that memory-related alpha power decreases are unlikely to be a consequence of reactivation and instead leaves the door open to them playing a causal role in supporting information representation (Hanslmayr et al., 2012, 2016; Michelmann et al., 2022) and/or conscious awareness (Mathewson et al., 2009; Benwell et al., 2021).

Total alpha power decreases paired with stimulus-specific rhythmicity additively predict overt recall of reactivated episodic memories

Finally, we investigated the extent to which stimulus-specific rhythmic reactivation and total alpha power decreases interact to predict overt recall. To do so, memory-related changes in total alpha power and stimulus-specific rhythmic reactivation were extracted and used as predictors together with an interaction term in a multiple linear regression that sought to predict memory performance. Memory performance could be predicted by both a decrease in total alpha power ($t_{(30)} = -2.30$; $p = 0.029$) and an increase in stimulus-specific rhythmic reactivation ($t_{(30)} = 2.99$; $p = 0.006$), but no interaction between these two measures was observed ($t_{(30)} = 0.82$; $p = 0.421$; Fig. 4). These results suggest that decreases in total alpha power and increases in stimulus-specific rhythmic reactivation independently and additively contribute to overt recall.

Discussion

Episodic memories are seen as inherently conscious entities (Tulving, 1985, 2002), yet growing evidence suggests that neural markers of episodic memory can be decoupled from consciousness (Henke et al., 2003; Hannula and Ranganath, 2009;

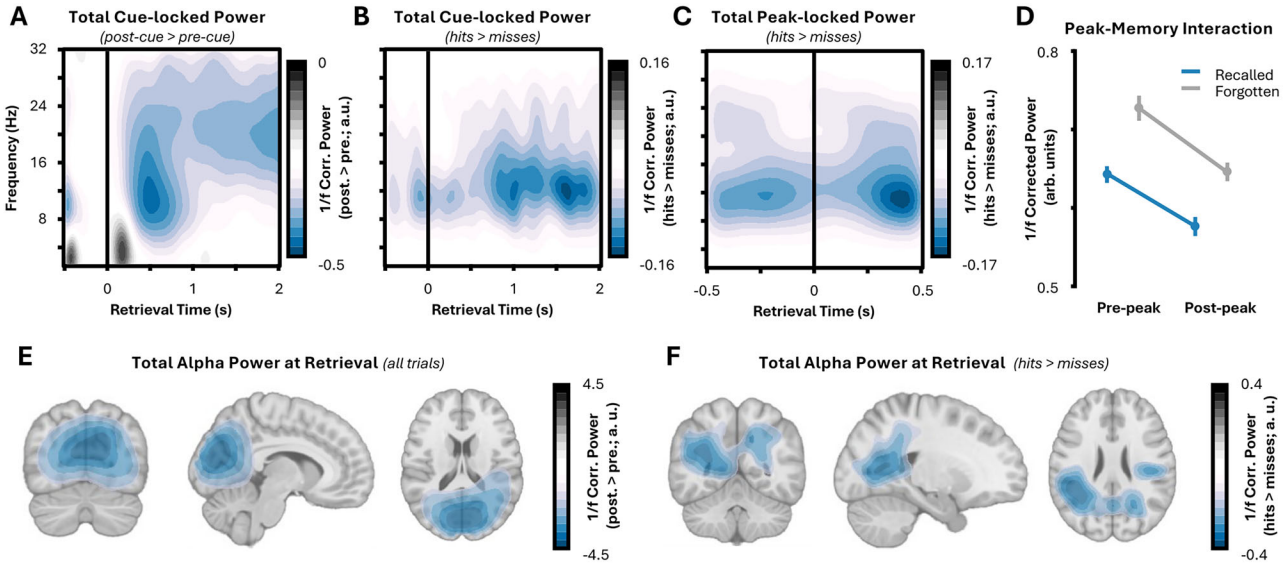


Figure 3. Overt recall is accompanied by a reduction in total alpha power. ***A***, Stimulus-induced changes in narrowband power. Alpha and beta power decreases occurs after the onset of the retrieval cue (time, 0 s). Time relative to the retrieval cue is presented on the *x*-axis; frequencies presented on the *x*-axis. The color bar depicts changes in power relative to prestimulus (−0.25 s to 0 s) activity. ***B***, Memory-related changes in narrowband power. Overt recall sees a greater reduction in alpha power relative to trials where the stimulus was not overtly recalled. Time relative to the retrieval cue is presented on the *x*-axis; frequencies presented on the *x*-axis. The color bar depicts changes in power for recalled relative to forgotten items. ***C***, Memory-related changes in narrowband power relative to decoding peak. Overt recall sees a greater reduction in alpha power relative to trials where the stimulus was not overtly recalled both before and after the moment of peak stimulus-specific decoding. Time relative to peak decoding is presented on the *x*-axis; frequencies presented on the *x*-axis. The color bar as in Panel ***B***. ***D***, No interaction between overt recall and peak-related alpha power changes. For both recalled (blue line) and forgotten items (dotted gray line), a decrease in alpha power is observed following the peak in decoding, but no interaction was observed between memory and the arrival of the peak. 1/*f*-corrected alpha power is presented on the *y*-axis, for each memory and peak condition separately. ***E***, Source localization of cue-induced alpha power decreases across all trials. Individual alpha peaks were determined for each participant based on prestimulus activity, and the resultant cue-induced power decrease was plotted for each source-localized virtual sensor. Voxels with values between 25% of the color bar minimum and 25% of the color bar maximum (here, −1.13 < voxel < 1.13) are masked. ***F***, Source localization of cue-induced alpha power decreases for hits relative to misses. Individual alpha peaks were determined for each participant based on prestimulus activity, and then memory-related change poststimulus alpha power was plotted for each source-localized virtual sensor. Voxels with values between 25% of the color bar minimum and 25% of the color bar maximum (here, −0.1 < voxel < 0.1) are masked.

Simons et al., 2010, 2022; Yazar et al., 2014; Ciaramelli et al., 2017; Schneider et al., 2021; Kolisnyk et al., 2025; Willems et al., 2025). This begs the question: how do we become aware of a reactivated memory? We find that while stimulus-specific content can be reactivated without overt recall, overt recall becomes more probable when reactivation is highly rhythmic. We speculate that this rhythmicity, occurring against a background of global alpha power decreases, marks the transition of a memory.

Prior research has demonstrated that key regions of the memory network (e.g., the hippocampus; Hannula and Ranganath, 2009; Willems et al., 2025) are active during unconscious recall of episodic memories, but it has remained unclear whether stimulus-specific representations can reactivate without inherently resulting in conscious awareness and/or overt recall. Our results suggest stimulus-specific content can indeed be reactivated across occipital/parietal regions in the absence of overt recall. Notably, a growing number of studies indicate that sensory reactivation in these regions occurs after hippocampal reactivation (Bosch et al., 2014; Griffiths et al., 2019b; Pacheco Estefan et al., 2019; Vaz et al., 2019) and gist-like reinstatement in deeper neocortical regions (Linde-Domingo et al., 2019; Lifanov-Carr et al., 2024). Therefore, one could speculate that none of these forms of reactivation guarantees overt recall. This highlights a separation between the neural mechanisms of reactivation and those of conscious awareness.

Instead, overt recall is predicted by reactivated memories being rhythmically represented in alpha oscillatory activity. This aligns with recent studies demonstrating that internally generated stimulus content is rhythmically represented in alpha oscillations (Michelmann et al., 2016; Kerrén et al., 2018; Noah et al., 2020; Xie et al., 2020; Chen et al., 2023; Stecher and Kaiser, 2024; Hetenyi et al., 2025) and that the magnitude of this rhythmicity predicts behavioral performance (Noah et al., 2020; Hetenyi et al., 2025). Intriguingly, the observation that alpha oscillations play an active role in information representation contradicts established views of alpha as an idling (Pfurtscheller et al., 1996) or inhibitory (Klimesch et al., 2007; Jensen and Mazaheri, 2010) rhythm. A potential explanation for this is that accounts of inhibition have principally been derived from studies of external perception and attention rather than on internally generated content such as episodic memory representations. Given recent proposals of frequency-specific information routing (Bastos et al., 2015, 2020; Miller et al., 2018; Stecher et al., 2025), where external information is fed forward by gamma oscillations and internal information is fed back by alpha/beta oscillations, one could argue for a fundamentally different role for alpha in the processing of external and internal stimulus representations, where alpha facilitates the representation of all manner of internally generated content while (or by) inhibiting the representation of externally perceived content (Miller et al., 2018).

The claim that reactivation can occur without overt recall may appear to contradict past work reporting differences in reactivation between remembered and forgotten information (Yaffe et al., 2014; Zhang et al., 2015; Jang et al., 2017; Liang and Preston, 2017; Pacheco Estefan et al., 2019). We believe, however, that this is not the case. Remembered versus forgotten contrasts assess whether "greater" reactivation predicts overt recall, while the forgotten versus zero contrasts reported above assess whether "any" reactivation predicts overt recall. In this light, the statistical results reported here can coexist with past findings: reactivation can occur without overt recall (i.e., the significant reactivation for forgotten items relative to chance observed here), but when reactivation is sufficiently strong, overt recall can occur (hence the significant difference in reactivation between remembered and forgotten items reported here and previously). Based on these findings, we speculate that reactivation must exceed a nonzero threshold to enter awareness rather than any degree of reactivation being satisfactory (Fig. 5).

Moreover, that stimulus-specific rhythmic reactivation occurs within the alpha band might seem to contradict past research linking alpha desynchronization to recall (Michelmann et al., 2016; Staresina et al., 2016; Waldhauser et al., 2016; Griffiths et al., 2019a,b; Karlsson et al., 2020; Martín-Buro et al., 2020; Griffiths et al., 2021; Katerman et al., 2022). However, our linear modeling results resolve this paradox, showing that global desynchronization and stimulus-specific rhythmic reactivation independently and additively predict overt recall. This statistical independence suggests these are dissociable phenomena: the rhythmic reactivation is unlikely to be a simple byproduct of the magnitude of alpha desynchronization itself. These separable

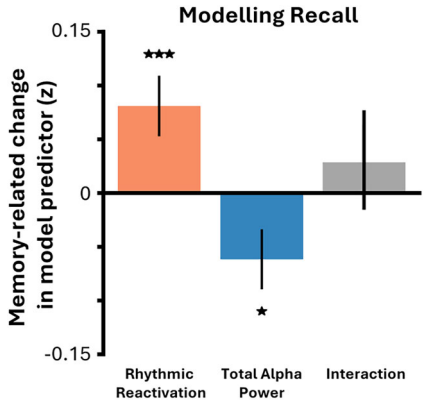


Figure 4. Total alpha power decreases paired with stimulus-specific rhythmic reactivation additively contribute to conscious awareness of reactivation episodic memories. Multiple linear regression predicting memory performance across participants. Stimulus-specific rhythmic reactivation, total alpha power, and their interaction were used to predict mean memory performance across participants. While stimulus-specific rhythmic reactivation and total alpha power both predicted mean memory performance, their interaction did not, suggesting they have separate, additive influences on memory. $*p < 0.05$; $***p < 0.005$.

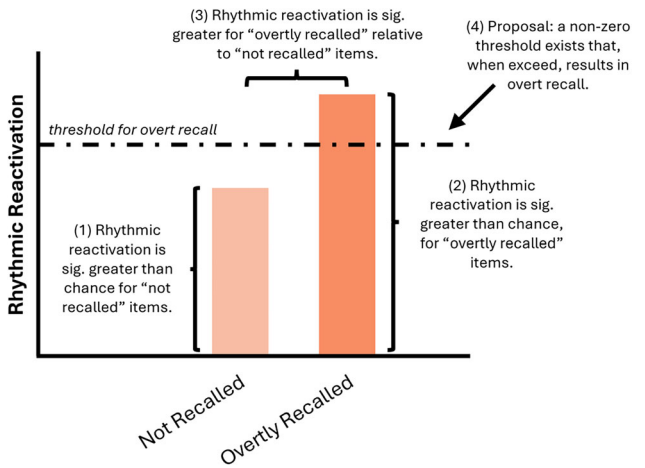


Figure 5. Conceptual figure visualizing key reactivation results. Statements 1–3 summarize the statistics results uncovered in the analyses presented in this paper. Statement 4 speculates as to why greater (as opposed to any) reactivation correlates with overt recall.

effects can be explained by multiple theoretical frameworks. For example, alpha power decreases could provide greater representational space for complex stimulus processing (Hanslmayr et al., 2012; Jensen et al., 2012), with stimulus-specific rhythmic reactivation being the most efficient means to transmit these codes across regions (Fries, 2015; Bastos et al., 2020). Alternatively, alpha power decreases and stimulus-specific rhythmic reactivation may reflect independent but complementary mechanisms to raise stimulus-specific content above task-irrelevant noise: alpha power decreases could reduce "noise correlations" from task-irrelevant assemblies, while stimulus-specific rhythmic reactivation amplifies task-relevant information (Griffiths et al., 2019a; Michelmann et al., 2022). Further research is required to more distinguish these possibilities. Regardless of theoretical interpretation, our results suggest that delineating different forms of alpha response may be key to understanding how these rhythms contribute to episodic memory.

These results focus on how memories recalled in response to a cue may be projected into awareness, but it is open to debate whether these findings generalize to other forms of episodic memory retrieval. For example, reactivation is less important in recognition/familiarity tests as the to-be-remembered information is presented to the participant during the memory test, rendering mechanisms that project reactivated content into awareness superfluous. Notably, while some elements of recognition/familiarity may play a role in our task (i.e., during the stimulus lineup following the recall window), they likely diminish the size of our effects rather than exaggerate them. Recognizing the stimulus but not reactivating it during the cue would result in a correct behavioral response without an accompanying neural representation, shrinking the mean representational strength for "correct" trials but having no impact on measures of representational strength for forgotten trials. Consequently, "recognition without recall" does not explain why forgotten items can be decoded better than expected by chance nor why recalled and forgotten items can be distinguished based on the rhythmicity of decoding. Nonetheless, exploring new experimental designs that better distinguish between the neural processes of reactivation, recall, and recognition may help pinpoint exactly how the brain projects memories into conscious awareness and, ultimately, help develop a more holistic explanation of conscious awareness in episodic memory retrieval.

The observation that overt recall can be decoupled from reactivation has important implications for clinical studies of, and interventions for, memory disorders. Specifically, our results suggest that neural interventions focused on facilitating reactivation would not reliably restore memory function as they cannot guarantee that the reactivated memory enters conscious awareness. Indeed, this may explain heterogeneity in outcomes for numerous promising memory interventions (Clouter et al., 2017; Martorell et al., 2019; Soula et al., 2023; Serin et al., 2024), and why even targeted reactivation of hippocampal memories cannot guarantee memory-guided behavioral responses (Liu et al., 2012). Speculatively, much could be gained by developing neuromodulatory techniques that focus on projecting reactivated memories into conscious awareness.

This study was not designed to adjudicate between neuroscientific theories of consciousness but nonetheless offers indirect insights into the neural dynamics of conscious awareness. For example, our findings generalize the link between alpha oscillations and conscious awareness from visual perception (Busch et al., 2009; Mathewson et al., 2009; Dugué et al., 2011; Spaak et al., 2014; Benwell et al., 2021; Griffiths et al., 2022; Fakche and Dugué, 2024) to internally generated visual content. Moreover, as this rhythmic effect is best explained by a neural code distributed across the cortex, it supports theories of consciousness emphasizing the importance of globally representing stimulus information [e.g., global neuronal workspace theory (Baars, 2005; Dehaene and Changeux, 2011; Mashour et al., 2020; Baars et al., 2021); higher order theory (Lau and Rosenthal, 2011; Brown et al., 2019); integrated information theory (Tononi et al., 2016; Albantakis et al., 2023)]. While this specific experimental design would struggle to further differentiate the nuances of specific theories of consciousness, it nonetheless demonstrates the benefits of using episodic memory as a source of internally generated stimuli to understand the neural correlates of consciousness.

In summary, these results suggest that conscious access to memory relies on a separable set of neural mechanisms from those related to neural reinstatement/reactivation. This suggests that a lack of conscious access can explain retrieval failure, offering new targets for neurocognitive interventions that augment memory and new insights into the oscillatory mechanisms that may be key to projecting memories into conscious awareness.

References

Albantakis L, et al. (2023) Integrated information theory (IIT) 4.0: formulating the properties of phenomenal existence in physical terms. PLoS Comput Biol 19:e1011465.

Baars BJ (2005) Global workspace theory of consciousness: toward a cognitive neuroscience of human experience. Prog Brain Res 150:45–53.

Baars BJ, Geld N, Kozma R (2021) Global workspace theory (GWT) and prefrontal cortex: recent developments. Front Psychol 12:749868.

Bainbridge WA, Walther DB, Fukuda K, Goetschalckx L (2025) Memorability of visual stimuli and the role of processing efficiency. Nat Rev Psychol 5: 47–58.

Bastos AM, Vezoli J, Bosman CA, Schoffelen J-M, Oostenveld R, Dowdall JR, De Weerd P, Kennedy H, Fries P (2015) Visual areas exert feedforward and feedback influences through distinct frequency channels. Neuron 85:390–401.

Bastos AM, Lundqvist M, Waite AS, Kopell N, Miller EK (2020) Layer and rhythm specificity for predictive routing. Proc Natl Acad Sci U S A 117: 31459–31469.

Benwell CSY, Coldea A, Harvey M, Thut G (2021) Low pre-stimulus EEG alpha power amplifies visual awareness but not visual sensitivity. Eur J Neurosci 55:3125.

Bosch SE, Jehee JFM, Fernández G, Doeller CF (2014) Reinstatement of associative memories in early visual cortex is signaled by the hippocampus. J Neurosci 34:7493–7500.

Brown R, Lau H, LeDoux JE (2019) Understanding the higher-order approach to consciousness. Trends Cogn Sci 23:754–768.

Busch NA, Dubois J, VanRullen R (2009) The phase of ongoing EEG oscillations predicts visual perception. J Neurosci 29:7869–7876.

Charles L, King J-R, Dehaene S (2014) Decoding the dynamics of action, intention, and error detection for conscious and subliminal stimuli. J Neurosci 34:1158–1170.

Chen L, Cichy RM, Kaiser D (2023) Alpha-frequency feedback to early visual cortex orchestrates coherent naturalistic vision. Sci Adv 9:1–10.

Ciaramelli E, Faggi G, Scarpazza C, Mattioli F, Spaniol J, Ghetti S, Moscovitch M (2017) Subjective recollection independent from multifeatural context retrieval following damage to the posterior parietal cortex. Cortex 91:114–125.

Clouter A, Shapiro KL, Hanslmayr S (2017) Theta phase synchronization is the glue that binds human associative memory. Curr Biol 27:1–6.

Dale AM, Fischl B, Sereno MI (1999) Cortical surface-based analysis. Neuroimage 9:179–194.

Dehaene S, Changeux J-P (2011) Experimental and theoretical approaches to conscious processing. Neuron 70:200–227.

Destrieux C, Fischl B, Dale A, Halgren E (2010) Automatic parcellation of human cortical gyri and sulci using standard anatomical nomenclature. Neuroimage 53:1–15.

Donoghue T, et al. (2020) Parameterizing neural power spectra into periodic and aperiodic components. Nat Neurosci 23:1655–1665.

Dugué L, Marque P, VanRullen R (2011) The phase of ongoing oscillations mediates the causal relation between brain excitation and visual perception. J Neurosci 31:11889–11893.
Fakche C, Dugué L (2024) Perceptual cycles travel across retinotopic space. J Cogn Neurosci 36:200–216.
Ferrante O, Liu L, Minarik T, Gorska U, Ghafari T, Luo H, Jensen O (2022) FLUX: a pipeline for MEG analysis. Neuroimage 253:119047.
Fries P (2015) Rhythms for cognition: communication through coherence. Neuron 88:220–235.
Gelbard-Sagiv H, Mukamel R, Harel M, Malach R, Fried I (2008) Internally generated reactivation of single neurons in human hippocampus during free recall. Science 322:96–101.
Gramfort A (2013) MEG and EEG data analysis with MNE-python. Front Neurosci 7:1–13.
Griffiths BJ, Mayhew SD, Mullinger KJ, Jorge J, Charest I, Wimber M, Hanslmayr S (2019a) Alpha/beta power decreases track the fidelity of stimulus-specific information. Elife 8:1–22.
Griffiths BJ, et al. (2019b) Directional coupling of slow and fast hippocampal gamma with neocortical alpha/beta oscillations in human episodic memory. Proc Natl Acad Sci U S A 166:21834–21842.
Griffiths BJ, Martín-Buro MC, Staresina BP, Hanslmayr S, Staudigl T (2021) Alpha/beta power decreases during episodic memory formation predict the magnitude of alpha/beta power decreases during subsequent retrieval. Neuropsychologia 153:107755–107755.
Griffiths BJ, Zaehle T, Repplinger S, Schmitt FC, Voges J, Hanslmayr S, Staudigl T (2022) Rhythmic interactions between the mediodorsal thalamus and prefrontal cortex precede human visual perception. Nat Commun 13:1–11.
Griffiths BJ, Duecker K, Fakche C, Dugué L, Quinn A, Jensen O (2025) Rhythmic light stimulation elicits multiple concurrent neural responses that separably shape human perception. *bioRxiv*.
Hannula DE, Ranganath C (2009) The eyes have It: hippocampal activity predicts expression of memory in eye movements. Neuron 63:592–599.
Hanslmayr S, Staudigl T, Fellner M-C (2012) Oscillatory power decreases and long-term memory: the information via desynchronization hypothesis. Front Hum Neurosci 6:1–12.
Hanslmayr S, Staresina BP, Bowman H (2016) Oscillations and episodic memory – addressing the synchronization/desynchronization conundrum. Trends Neurosci 39:16–25.
Henke K, Treyer V, Nagy ET, Kneifel S, Dürsteler M, Nitsch RM, Buck A (2003) Active hippocampus during nonconscious memories. Conscious Cogn 12:31–48.
Hetenyi D, Haarsma J, Kok P (2025) Contents of visual predictions oscillate at alpha frequencies. J Neurosci 45:e0474252025.
Holmes CJ, Hoge R, Collins L, Woods R, Toga AW, Evans AC (1998) Enhancement of MR images using registration for signal averaging. J Comput Assist Tomogr 22:324–333.
Jang AI, Wittig JH, Inati SK, Zaghloul KA (2017) Human cortical neurons in the anterior temporal lobe reinstate spiking activity during verbal memory retrieval. Curr Biol 27:1700–1705.e5.
Jensen O, Mazaheri A (2010) Shaping functional architecture by oscillatory alpha activity: gating by inhibition. Front Hum Neurosci 4:1–8.
Jensen O, Bonnefond M, VanRullen R (2012) An oscillatory mechanism for prioritizing salient unattended stimuli. Trends Cogn Sci 16:200–206.
Karlsson AE, Wehrspaun CC, Sander MC (2020) Item recognition and lure discrimination in younger and older adults are supported by alpha/beta desynchronization. Neuropsychologia 148:107658.
Katerman BS, Li Y, Pazdera JK, Keane C, Kahana MJ (2022) EEG biomarkers of free recall. Neuroimage 246:118748.
Kerrén C, Linde-Domingo J, Hanslmayr S, Wimber M (2018) An optimal oscillatory phase for pattern reactivation during memory retrieval. Curr Biol 28:3383–3392.e6.
Kerrén C, van Bree S, Griffiths BJ, Wimber M (2023) Phase separation of competing memories along the human hippocampal theta rhythm. Elife 11:1–26.
Kerrén C, Zhao Y, Griffiths BJ (2024) A reduction in self-reported confidence accompanies the recall of memories distorted by prototypes. Commun Psychol 2:1–11.
Kerrén C, Reznik D, Doeller CF, Griffiths BJ (2025) Exploring the role of dimensionality transformation in episodic memory. Trends Cogn Sci 29:614–626.
King J-R, Pescetelli N, Dehaene S (2016) Brain mechanisms underlying the brief maintenance of seen and unseen sensory information. Neuron 92: 1122–1134.
Klimesch W, Sauseng P, Hanslmayr S (2007) EEG alpha oscillations: the inhibition-timing hypothesis. Brain Res Rev 53:63–88.
Kolisnyk M, Laforge G, Gagnon M-È, Erez J, Owen AM (2025) Total recall: detecting autobiographical memory retrieval in the absence of behaviour. Neuropsychologia 211:109129.
Kriegeskorte N, Simmons WK, Bellgowan PSF, Baker CI (2009) Oost. Nat Neurosci 12:535–540.
Kyle-Davidson C, Bors AG, Evans KK (2022) Modulating human memory for complex scenes with artificially generated images. Sci Rep 12:1583.
Lau H, Rosenthal D (2011) Empirical support for higher-order theories of conscious awareness. Trends Cogn Sci 15:365–373.
Liang JC, Preston AR (2017) Medial temporal lobe reinstatement of content-specific details predicts source memory. Cortex 91:67–78.
Lifanov-Carr J, Griffiths BJ, Linde-Domingo J, Ferreira CS, Wilson M, Mayhew SD, Charest I, Wimber M (2024) Reconstructing spatiotemporal trajectories of visual object memories in the human brain. eNeuro 11: ENEURO.0091-24.2024.
Linde-Domingo J, Treder MS, Kerrén C, Wimber M (2019) Evidence that neural information flow is reversed between object perception and object reconstruction from memory. Nat Commun 10:1–13.
Liu X, Ramirez S, Pang PT, Puryear CB, Govindarajan A, Deisseroth K, Tonegawa S (2012) Optogenetic stimulation of a hippocampal engram activates fear memory recall. Nature 484:381–385.
Maris E, Oostenveld R (2007) Nonparametric statistical testing of EEG- and MEG-data. J Neurosci Methods 164:177–190.
Martín-Buro MC, Wimber M, Henson RN, Staresina BP (2020) Alpha rhythms reveal when and where item and associative memories are retrieved. J Neurosci 40:2510–2518.
Martorell AJ, et al. (2019) Multi-sensory gamma stimulation ameliorates Alzheimer's-associated pathology and improves cognition. Cell 177: 256–271.e22.
Mashour GA, Roelfsema P, Changeux J-P, Dehaene S (2020) Conscious processing and the global neuronal workspace hypothesis. Neuron 105:776–798.
Mathewson KE, Gratton G, Fabiani M, Beck DM, Ro T (2009) To see or not to see: prestimulus α phase predicts visual awareness. J Neurosci 29:2725–2732.
Michelmann S, Bowman H, Hanslmayr S (2016) The temporal signature of memories: identification of a general mechanism for dynamic memory replay in humans. PLoS Biol 14:e1002528.
Michelmann S, Griffiths B, Hanslmayr S (2022) The role of alpha and beta oscillations in the human EEG during perception and memory processes. In: *The Oxford handbook of EEG frequency* (Gable PA, Miller MW, Bernat EM, eds), Ed 1. pp 202–219. UK: Oxford University Press.
Miller EK, Lundqvist M, Bastos AM (2018) Working memory 2.0. Neuron 100:463–475.
Miller KJ, Sorensen LB, Ojemann JG, Den Nijs M (2009) Power-law scaling in the brain surface electric potential. PLoS Comput Biol 5:1–10.
Moscovitch M, Cabeza R, Winocur G, Nadel L (2016) Episodic memory and beyond: the hippocampus and neocortex in transformation. Annu Rev Psychol 67:105–134.
Noah S, Powell T, Khodayari N, Olivan D, Ding M, Mangun GR (2020) Neural mechanisms of attentional control for objects: decoding EEG alpha when anticipating faces, scenes,and tools. J Neurosci 40: 4913–4924.
Pacheco Estefan D, Sánchez-Fibla M, Duff A, Principe A, Rocamora R, Zhang H, Axmacher N, Verschure PFMJ (2019) Coordinated representational reinstatement in the human hippocampus and lateral temporal cortex during episodic memory retrieval. Nat Commun 10:2255–2255.
Pedregosa F, et al. (2011) Scikit-learn: machine learning in python. J Mach Learn Res 12:2825–2830.
Pfurtscheller G, Stancák A, Neuper C (1996) Event-related synchronization (ERS) in the alpha band—an electrophysiological correlate of cortical idling: a review. Int J Psychophysiol 24:39–46.
Schneider E, Züst MA, Wuethrich S, Schmidig F, Klöppel S, Wiest R, Ruch S, Henke K (2021) Larger capacity for unconscious versus conscious episodic memory. Curr Biol 31:3551–3563.e9.
Serin F, Wang D, Davis MH, Henson R (2024) Does theta synchronicity of sensory information enhance associative memory? Replicating the theta-induced memory effect. Brain Neurosci Adv 8:1–7.
Simons JS, Peers PV, Mazuz YS, Berryhill ME, Olson IR (2010) Dissociation between memory accuracy and memory confidence following bilateral parietal lesions. Cereb Cortex 20:479–485.

Simons JS, Ritchey M, Fernyhough C (2022) Brain mechanisms underlying the subjective experience of remembering. Annu Rev Psychol 73:159–186.
Singer AC, Frank LM (2009) Rewarded outcomes enhance reactivation of experience in the hippocampus. Neuron 64:910–921.
Soula M, Martín-Ávila A, Zhang Y, Dhingra A, Nitzan N, Sadowski MJ, Gan W-B, Buzsáki G (2023) Forty-hertz light stimulation does not entrain native gamma oscillations in Alzheimer's disease model mice. Nat Neurosci 26:570–578.
Spaak E, de Lange FP, Jensen O (2014) Local entrainment of alpha oscillations by visual stimuli causes cyclic modulation of perception. J Neurosci 34: 3536–3544.
Staresina BP, Wimber M (2019) A neural chronometry of memory recall. Trends Cogn Sci 23:1071–1085.
Staresina BP, Alink A, Kriegeskorte N, Henson RN (2013) Awake reactivation predicts memory in humans. Proc Natl Acad Sci U S A 110:21159–21164.
Staresina BP, Michelmann S, Bonnefond M, Jensen O, Axmacher N, Fell J (2016) Hippocampal pattern completion is linked to gamma power increases and α power decreases during recollection. Elife 5:1–18.
Staresina BP, Reber TP, Niediek J, Boström J, Elger CE, Mormann F (2019) Recollection in the human hippocampal-entorhinal cell circuitry. Nat Commun 10:1503.
Stecher R, Kaiser D (2024) Representations of imaginary scenes and their properties in cortical α activity. Sci Rep 14:12796.
Stecher R, Cichy RM, Kaiser D (2025) Decoding the rhythmic representation and communication of visual contents. Trends Neurosci 48:178–188.
Tayler KK, Tanaka KZ, Reijmers LG, Wiltgen BJ (2013) Reactivation of neural ensembles during the retrieval of recent and remote memory. Curr Biol 23:99–106.
Teyler TJ, Rudy JW (2007) The hippocampal indexing theory and episodic memory: updating the index. Hippocampus 17:1158–1169.
Thakral PP, Wang TH, Rugg MD (2015) Cortical reinstatement and the confidence and accuracy of source memory. Neuroimage 109:118–129.
Tononi G, Boly M, Massimini M, Koch C (2016) Integrated information theory: from consciousness to its physical substrate. Nat Rev Neurosci 17:450–461.
Tsuchiya N, Wilke M, Frässle S, Lamme VAF (2015) No-report paradigms: extracting the true neural correlates of consciousness. Trends Cogn Sci 19:757–770.
Tulving E (1985) Memory and consciousness. Can Psychol 26:1–12.
Tulving E (2002) Episodic memory: from mind to brain. Annu Rev Psychol 53:1–25.
Van Bree S, Mackenzie AS, Wimber M (2024) No evidence that visual impulses enhance the readout of retrieved long-term memory contents from EEG activity. Imag Neurosci 2:1–16.
Vaz AP, Inati SK, Brunel N, Zaghloul KA (2019) Coupled ripple oscillations between the medial temporal lobe and neocortex retrieve human memory. Science 363:975–978.
Waldhauser GT, Braun V, Hanslmayr S (2016) Episodic memory retrieval functionally relies on very rapid reactivation of sensory information. J Neurosci 36:251–260.
Willems T, Zervas K, Rabe F, Federspiel A, Henke K (2025) Neural Traces of Forgotten Memories Persist in Humans and are Behaviorally Relevant. *bioRxiv*.
Wilson MA, McNaughton BL (1994) Reactivation of hippocampal ensemble memories during sleep. Science 265:676–679.
Xie S, Kaiser D, Cichy RM (2020) Visual imagery and perception share neural representations in the alpha frequency band. Curr Biol 30:2621–2627.e5.
Yaffe RB, Kerr MSD, Damera S, Sarma SV, Inati SK, Zaghloul KA (2014) Reinstatement of distributed cortical oscillations occurs with precise spatiotemporal dynamics during successful memory retrieval. Proc Natl Acad Sci U S A 111:18727–18732.
Yazar Y, Bergström ZM, Simons JS (2014) Continuous theta burst stimulation of angular gyrus reduces subjective recollection. PLoS One 9:e110414.
Zhang H, Fell J, Staresina BP, Weber B, Elger CE, Axmacher N (2015) Gamma power reductions accompany stimulus-specific representations of dynamic events. Curr Biol 25:635–640.